Three–dimensional inversion of time–domain EM data with highly constrained model complexities

Michael Commer[1], Andreas Hördt[2], Stefan L. Helwig[1], Carsten Scholl[1]

Abstract

The standard one–dimensional (1D) inversion approach for the interpretation of transient electromagnetic (TEM) data may fail or lead to misinterpretation if a more complex underground structure or topography is present. However, the solution of a full three–dimensional (3D) electromagnetic inverse problem is non–trivial because usually it is very large in scale. This results from the usual practice of representing the underground by a large number of discrete grid cells to account for model parameter variations in all three Cartesian dimensions. Here, an alternative 3D inversion approach that strongly constrains the earth model is presented. The idea of the scheme is the combination of a Marquardt–Levenberg method as a stable inversion scheme with an existing 3D forward modeling code. The approach addresses the large–scale difficulty by limiting the number of model unkowns to as many unknowns as typical for Marquardt inversions. To describe a 3D earth with few model parameters involves alternative types of model unknowns, which need to be adapted to the structures of interest before an inversion is started. This makes the knowledge of a priori information a requirement for the presented inversion method.

Introduction

In the geophysical literature, a large number of examples can be found for EM surveys, which are characterized as follows:

1. The collected data are insufficient for resolving a numerous set of model unknowns in a large–scale inversion approach. This may have several reasons, where logistic and / or economic limitations might be dominant. In other cases, a survey may have the aim of a preliminary investigation of a target and thus involves only a limited amount of measurements.

2. There exists prior knowledge about the target. This can be given by other geophysical disciplines, geological information or borehole measurements. In many cases, TEM surveys are carried out on the basis of a priori information in order to refine the model of an a priori known target, for examples refer to Taylor et al. (1992); Hördt et al. (2000).

3. Simplified 1D inversion approaches fail to take multi–dimensional effects contained in the data into account. Even if a data fit can be achieved, laterally biased interpretations can be expected when 1D methods are applied to the response of more complex structures. Examples where 1D inversions do not accurately recover 2D or 3D resistivtiy distributions are shown by Newman et al. (1987); Blohm et al. (1991); Christensen (2002).

While much work has already been done in dealing with the full 3D inversion of TEM data (Zhdanov and Frenkel, 1983; Wang et al., 1994; Mitsuhata et al., 2002; Zhdanov and Wannamaker, 2002), its computational expense still remains a major difficulty. The inversion method presented here is optimized for problems characterized by the above listed aspects. A Marquardt–Levenberg (Levenberg, 1944; Marquardt, 1963) method as a stable inversion scheme is combined with the 3D forward modeling code from Druskin and Knizhnerman (1988). The approach addresses the large–scale difficulty by limiting the number of model unkowns to as many unknowns as typical for Marquardt inversions. Inverting for a “low–parameterized” model involves an over–determined system to be solved. This provides for the capability of resolving multi–dimensional structures even if only a limited amount of field data is available.

The large–scale character of full 3D inversions originates from the usual practice of treating the discrete cells of a finite–difference or finite–element mesh as model unknowns. Such a fine model parameterization quickly leads to a huge set of parameters, but offers a maximum of degrees of freedom during an inversion. Here, this flexibility is sacrificed for computational efficiency by constraining the model variation such that the shape of the resistivity structure has to be

[1]Institute of Geophysics and Meteorology, University of Cologne, Germany
[2]Institute of Geology, Dept. of Applied Geophysics, University of Bonn, Germany

defined prior to an inversion. To describe a 3D earth, this involves alternative types of model unknowns, which need to be adapted to the structures of interest. Therefore, it is crucial that sufficient a priori information exists to define proper model parameters. Two examples for rather unconventional parameter types will be shown in the course of this article. The first one involves a synthetic data example, where the model unknowns represent the position of an anomaly. The second one presents an inversion of the Long–Offset TEM (LOTEM) (Strack, 1992) data from the volcano Merapi (Central–Java, Indonesia).

The inversion scheme has also been presented in an earlier article (Commer et al., 2001), where LOTEM data inversion results from Mount Merapi were shown. Here, we both show an additional synthetic data example for arbitrary model parameters and an improvement of the field data inversion of the LOTEM measurements from Merapi.

Methodology

The forward modeling code

The forward modeling code is based on the spectral Lanczos decomposition method (SLDM). The theory of this solution method is described by Druskin and Knizhnerman (1988, 1994); Druskin et al. (1999); a brief summary is also given by Hördt et al. (1992). The code solves the 3D diffusive Maxwell equations using finite differences (FD) and Krylov subspace techniques. Such techniques are very efficient for the solution of large linear systems with a sparse matrix arising from the FD discretization of a complex earth model [e.g. (Madden and Mackie, 1989; Alumbaugh et al., 1996; Smith, 1996)]. The SLDM code is practically unlimited in terms of model complexity. It allows an approximation of real geology by defining areas of constant conductivity in the form of rectangular blocks that do not necessarily conform to the FD grid. This is realized by a material averaging scheme to calculate the underlying effective medium (Moskow et al., 1999). This feature makes the code appropriate for the inversion scheme, because conductivity boundaries can be changed and moved without having to modify the FD grid.

It is crucial that the convergence characterisics of SLDM are taken into account when designing a FD discretization for a given earth model. Here, the most important aspects are outlined. A detailed and more theoretical description is given by Druskin and Knizhnerman (1994). The convergence of SLDM depends on the differential equation system's condition number, that is the ratio between largest and smallest eigenvalue. The condition number depends on the aspect ratio of a FD grid. Ill–conditioning due to a large condition number is introduced by high conductivity contrasts. This results from the requirement that for the application of SLDM the grid discretization should be fine in conductive regions and coarse in more resistive regions in order to achieve a proper simulation of the attenuation characteristics of EM fields. Hence, convergence problems may occur in the presence of high contrasts if a compromising grid discretization cannot be found. Furthermore, a fine grid should be used to ensure accurate results at early times, whereas low frequency fields need coarse spacings for a quick convergence (Druskin and Knizhnerman, 1994). Therefore, the simulation of late times also decrease the convergence due to large FD grid aspect ratios. For brevity, we refer to Commer (2003) for various methods that minimize convergence problems of the SLDM code in the presence of both large resistivity contrasts and low frequency fields.

The Marquardt–Levenberg inversion scheme

The Marquardt–Levenberg inversion scheme [e.g. Jupp and Vozoff (1975); Lines and Treitel (1984)] represents a stable iterative method in the presence of ill–posed inversion problems, where small changes in the data can lead to large changes in both the solution and in the process that finds the solution. The Marquardt correction step of an iteration is also related to the solution of the damped least–squares problem. Starting from a modified form of the normal equations Lines and Treitel (1984) derive the model correction quantity

$$\delta\mathbf{m} = (\mathbf{J}^T\mathbf{J} + \beta\mathbf{I})^{-1}\mathbf{J}^T\delta\mathbf{d}. \qquad (1)$$

The matrix $\mathbf{I}$ denotes the identity matrix and $\delta\mathbf{d}$ is the data misfit vector between observed data and the data prediction calculated by the current model of the iteration. The matrix $\mathbf{J}$ represents the partial derivatives of the predicted data with respect to the model parameters,

$$\mathbf{J}_{ij} = \frac{\partial d_i}{\partial m_j} \qquad i = 1, ..., N; \;\; j = 1, ..., M \qquad (2)$$

and is also referred to as parameter sensitivity matrix or Jacobian. The size of $\mathbf{J}$ is $N \times M$, given by the number of observed data points and the number of model unknowns, respectively.

The constant β controls the amount of damping of the solution and thus relieves the potential singularity of $\mathbf{J}^T\mathbf{J}$ by adding a constant to its main diagonal. Refer to Jupp and Vozoff (1975) for a detailed discussion of the damping factor. Here, we follow the damping scheme employed by Vozoff and Jupp (1975). In principal a threshold level is raised by the damping parameter in the first iteration so that only the basic features of the model will be resolved. A gradual decrease of β accounts for less resolved model parameters at later iterations. To define a stopping criteria for an inversion, a lower treshold for the relative decrease of $\delta\mathbf{d}$, with respect to the previous iteration, is chosen in advance.

The presence of data errors assigned to the observations is addressed by incorporating a weighting matrix $\mathbf{W}$ into the solution (1). Usually, $\mathbf{W}$ is a diagonal matrix, where its entries are the reciprocal values of the standard deviations of the measurements (Jackson, 1972). Incorporating the data weighting changes the solution in (1) to (Hördt, 1989)

$$\delta\mathbf{m} = (\mathbf{J}^T\mathbf{W}^2\mathbf{J} + \beta\mathbf{I})^{-1}\mathbf{J}^T\mathbf{W}^2\delta\mathbf{d}. \qquad (3)$$

The calculation of the sensitivity matrix $\mathbf{J}$ is usually the most time–consuming part of an inversion procedure, because this requires calculating the variation in the data produced by a change in the model parameters at each iteration. Elegant ways based on the adjoint equation method (McGillivray et al., 1994; Hördt, 1998) exist to calculate parameter sensitivities. These methods employ the reciprocity relationship and thus the computational effort is governed by the number of receiver stations of the inverted data rather than the number of unknowns. However, in our approach the small number of model parameters makes the perturbation method computationally competitive. It is accomplished by perturbing each model parameter separately by a finite quantity. The data response of both the perturbed and unperturbed model are then used to compute the differences of (2) yielding one column of the Jacobian for each perturbation.

The expensive calculation of the Jacobian can be highly accelerated if a parallel computing platform is used. As the forward simulations for the perturbed model parameters are carried out independently from each other, they can be distributed among several processors (Scholl et al., 2002).

Data and model parameter transformation

Diffusive EM fields have widely different amplitudes at different times and receiver locations. To reduce the dynamic range of the data, transformations are preferable in order to equalize the influence of each datum. Otherwise, the solution (1) may be dominated by high amplitude data points, thus deteriorating the convergence in an inversion (Meju, 1994). A simple logarithmic transformation (Jupp and Vozoff, 1975) can be used if all data points are of the same sign. However, TEM measurements over 3D structures often involve sign reversals over the measurement time range, thus requiring to distinguish between positive and negative data. Different methods exist to take both large amplitude variations and different signs into account. For example, Wang et al. (1994) use a logarithmic transformation with a linear scale straddling amplitudes near zero and a discrimination between positive and negative logarithms of data values. We use a transformation scheme that proved to be suitable for the 1D inversion of LOTEM data containing sign reversals[1] (Scholl, 2001). It is based upon the Area–Sinus–Hyperbolicus function. The funtion has a logarithmic behaviour for arguments $\gg 1$ or $\ll -1$ and a linear one for arguments close to zero.

An important constraint on model parameters such as for example electrical conductivity or layer thickness is that they must be positive quantities. To enforce this constraint on the inverse solution, a logarithmic transformation can be used. It also has the advantage of stabilizing the solution if any parameter becomes very small (Jupp and Vozoff, 1975). However, it may depend on the type of model unknowns which data transformation is appropriate. For example, consider a parameter describing the variable position of some model feature, as will be exemplified below. Depending on the specification of the FD grid, it may be necessary to allow negative values. However, one can avoid this complication by shifting the positions internally to the positive FD grid axes such that negative values never occur.

It needs to be taken into account that both data and model parameter transformations carry over to the calculation of the Jacobian in Equation (2). Furthermore, the data transformation affects the data errors and thus the weighting matrix $\mathbf{W}$. Scholl (2001) outlines these aspects in great detail for different types of transformations.

Results

Synthetic data example

In the following the inversion scheme is tested on a synthetic data set. The data for the tests is created using another FD code (Commer, 2003) in order to provide for independency from the SLDM code. No artificial noise is added to the data, because we want to simulated the case of an optimal data quality. The inversion of field data with realistic noise will be treated in the next section.

Consider the 3D model shown by the shaded rectangle in Figure 1a. The model represents a $1\ \Omega\cdot\mathrm{m}$ conductive cube embedded in a $50\ \Omega\cdot\mathrm{m}$ homogeneous half–space. The horizontal dimensions of the body are 200 m on a side with a vertical size of 140 m and its depth starting at 60 m. A horizontal grounded–wire source of length 80 m is located at 200 m distance to the left edge of the block. A single receiver is placed at 500 m distance to the transmitter. The simulated data comprises the electric field component in a direction parallel to the source orientation and the time derivative of the vertical magnetic induction.

It is assumed that the block's geometry is known and hence it is kept fixed during the inversion. Further-

[1] Depending on the LOTEM transmitter–receiver geometry and the type of the field component, sign reversals can occur over a 1D earth (Petry, 1987).

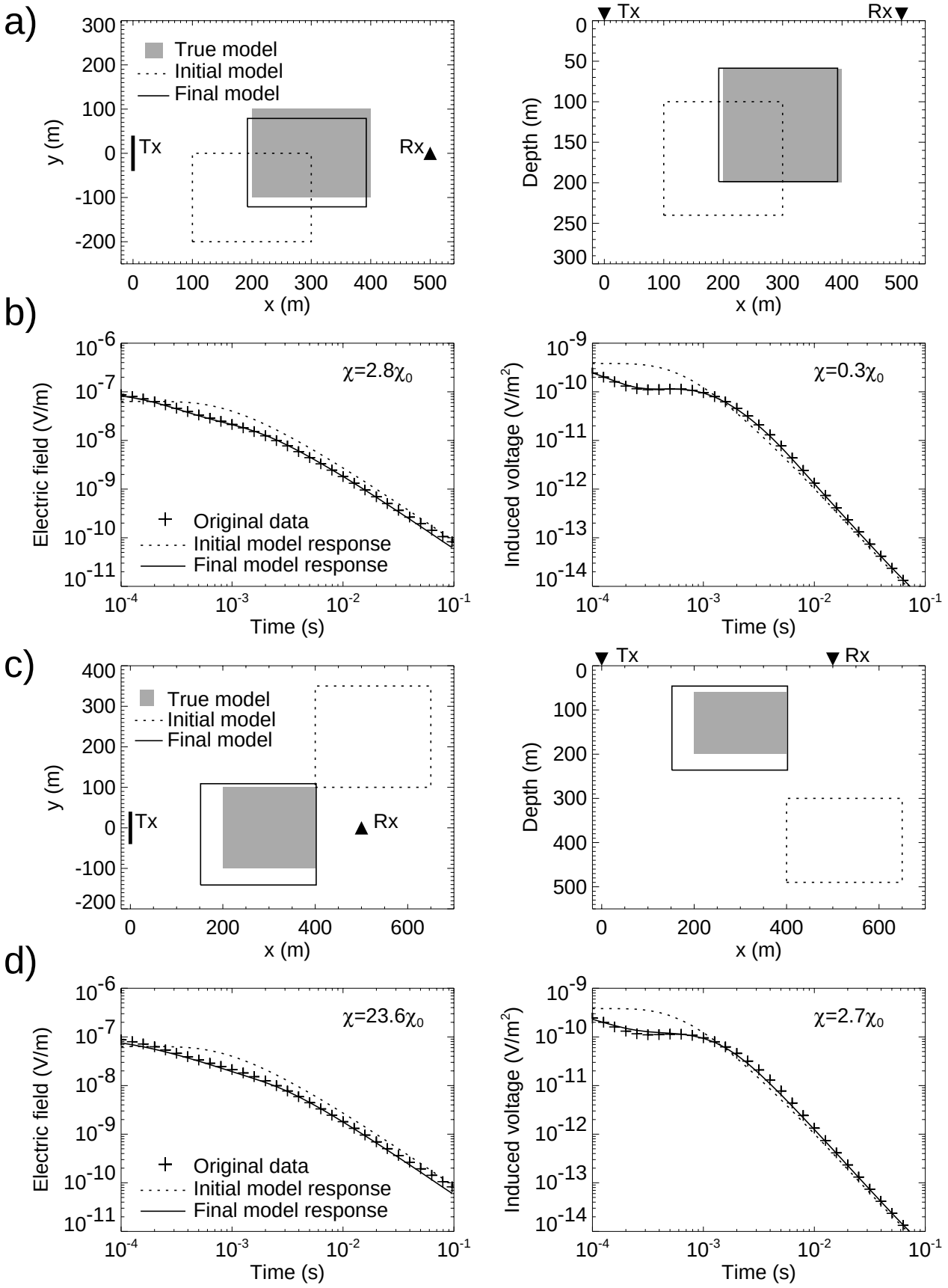

Figure 1: *Synthetic data inversion for the resistivity and position of a block embedded in a homogeneous half–space. (a) Plan view and vertical section of the true (shaded rectangle), initial (dashed lines) and final (solid lines) block position of an inversion with conforming block geometry. (b) Synthetic data calculated at the receiver (Rx) in comparison with initial and final model response for both inverted data sets. (c) Initial and final model results for an inversion with nonconforming block geometry and (d) corresponding data fits.*

more the half–space resistivity does not vary. While we are aware that this would represent a fairly detailed structural knowledge, both shall represent the a priori information for this model study. Four unknowns are defined, given by the block's resistivity and the positions x, y and z of its center. The starting model assumes a 50 $\Omega \cdot \mathrm{m}$ block and a 100 m offset from the true position for both horizontal coordinates x and y and a 40 m offset from the true depth (dashed rectangle).

The solid lines mark the resulting block location after 8 iterations. The inversion moves the initial block towards the original location (shaded rectangle) such that a good agreement along both the x axis and the vertical axis is achieved. The only significant deviation of approximately 20 m from the true position occurs along the y axis. The block's resistivity of 1 $\Omega \cdot \mathrm{m}$ is reproduced exactly in this example. For both data components Figure 1b shows the synthetic data generated by the original model in comparison with both the initial response and the response calculated from the solution. We use the sum of the squared differences between original and predicted data for a comparison of the data fits. This value, denoted as χ in Figure 1b, is given relative to the ideal fit χ_0, which is calculated from the true model. It can be observed that the electric field data fit is more sensitive to the slightly erroneous model reconstruction. For the magnetic field data, the resulting model achieves a better data fit than the true model, indicating that this data component provides a worse resolution than the electric field. This was also confirmed by further studies where both data components were inverted separately (Commer, 2003).

In order to exemplify another inversion with a less conforming parameterization, the block's geometry is now assumed to be 50 m larger along each dimension, as illustrated by the dashed rectangle in Figure 1c. Also, the starting position is shifted farther away from the true position, such that its center coordinates differ by values of $\Delta x = 225$ m, $\Delta y = 225$ m and $\Delta z = 265$ m from the true center point coordinates. The final model result reveals a successful inversion, because the real block is enclosed by the borders of the assumed block after 9 iterations. The larger block volume causes a trend towards the resistivity of the background. The initial block resistivity of 50 $\Omega \cdot \mathrm{m}$ is decreased to a value of 7.2 $\Omega \cdot \mathrm{m}$. To compare, this yields a product of conductivity and volume of $1.65 \cdot 10^6$ $\mathrm{S} \cdot \mathrm{m}^2$, whereas for the true block this product is $5.6 \cdot 10^6$ $\mathrm{S} \cdot \mathrm{m}^2$. Figure 1d shows a good agreement between the synthetic data and the response of the inversion result. In contrast to Figure 1b, one observes a slight misfit in the early time range of both data types. Again, the different degrees of resolution of each data type is indicated by the different values of χ calculated from the nonconforming model result.

A question to be further investigated is the kind of model parameter transformations used for such unconventional parameters as the position of an anomaly. Here, for simplicity a logarithmic transformation was used for all parameters and led to satisfying results. In order to avoid negative numbers for the block position parameters, the model domain was internally shifted to the positive FD grid axes. Instead, a different parameter transformation scheme could be used, which decides subject to the parameter type if a transformation is employed and what type of transformation function is used. For the presented example, a linear treatment of the position parameters is probably more appropriate, where a logarithmic one should be retained for resistivity parameters.

Field data example

The following example shows the inversion of LOTEM data from a survey conducted at the active volcano Merapi (Central–Java, Indonesia). Using the same inversion scheme, the inversion of LOTEM data measured at the summit region of Merapi has already been accomplished in an earlier article (Commer et al., 2001). In this article we present improved inversion results, because both more data and more model features are treated in the following approach.

The LOTEM project at Merapi was a part of a multidisciplinary cooperation of the German Science Foundation (DFG) and the Volcanological Survey of Indonesia (VSI). Zschau et al. (1998) presented an overview of all activities. LOTEM measurements were made during surveys in the years 1998, 2000 and 2001 and are described by Müller et al. (2002) and Commer et al. (2003) in more detail. The steep topography of the survey area was the main reason for logistical difficulties, thereby prohibiting a fast buildup of the receiver stations. Hence, instead of an area–wide covering of the target, measurements were made at single stations and along a limited number of profiles, where an access was possible. Furthermore, the data quality suffered from a high portion of noise at some stations, thus requiring long recording times in order to obtain satisfying signal–to–noise ratios. Other problems, such as frequent rainfall, also led to a deteriorated data quality at some stations. These difficulties are the reason for a limited amount of available data with sufficient quality for a 3D inversion.

The receivers of the inverted data were located on the northern, western and southern flanks and at the summit region. Their positions are shown in Figure 2. All inverted transients are the time derivatives of the magnetic induction. The surveys at Merapi also involved the measurement of electric fields. Unfortunately, most of the electric fields recorded at the shown stations were characterized by a poor quality. Electric fields are very susceptible to a poor galvanic coupling of the sensor electrode pairs (Helwig, pers.

comm.). This caused significant distortions, because most of the stations in the summit region and along the upper flanks were located on a dry and rocky ground.

The transmitter Tx1 used for Stations 1–6 had a bipole length of approximately 1 km and was located in the north at approximately 4 km distance from the summit at an elevation of 1500 m above sea level. Station 7 was measured at the same position as Station 1 using a different transmitter (Tx2) of 2 km length located at 530 m elevation and 12.8 km distance south from the summit region. Vertical field components are available at all shown receiver positions. In addition, horizontal components with sufficient data quality were recorded at Stations 4–6. Stations 3–6, 1–2 and 7 were measured during the 1998, 2000 and 2001 surveys, respectively. In addition to vertical fields, we present for the first time the inversion of horizontal components of the magnetic induction time derivative.

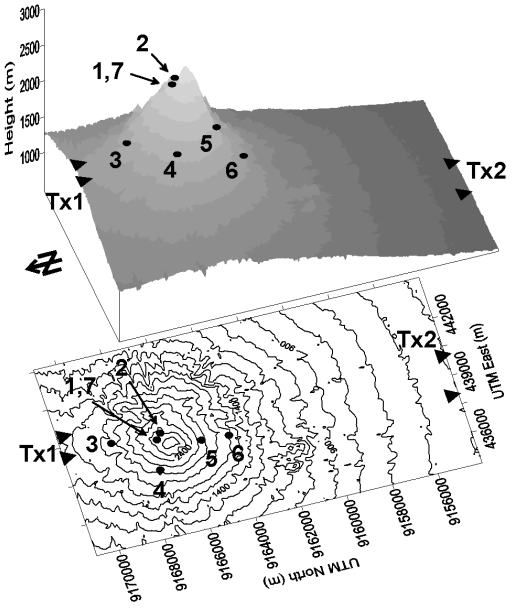

Figure 2: *Digital elevation model (Gerstenecker et al., 1998) and contour map of the survey area. Triangles mark the LOTEM transmitter electrode positions, circles mark receiver positions.*

We used a priori information from different disciplines in order to define an appropriate model parameterization. From 1D inversion results of LOTEM data (Müller et al., 2002) and DC resistivity modeling (Friedel et al., 2000), we know about the presence of a conductive layer below the volcanic edifice. Both disciplines found that the isoresistivity lines along profiles in a north–south direction nearly follow the topography. This was also observed for DC resistivity measurements along the western flank (Friedel et al., 2000). Furthermore, the models obtained from the fit of magnetotelluric induction vectors with periods from 0.1–10 seconds are in accordance with a conductor with an upwelling structure (Müller, 2000). The 3D MT forward modeling result includes topography and is characterized by a rising $10\,\Omega \cdot \mathrm{m}$ conductor located in the volcano's center. Both LOTEM and MT results suggest that the conductor starts at a depth of approximately 1000 m below the surface.

Since the conductive layer might be a simplification of a gradual resistivity decrease with depth, we allow a multi–layer model in the following inversion attempt. Similar to 1D inversions, the parameters are given by layer resistivities and thicknesses. A constraining condition is imposed such that the layers strictly follow the topography. As realized in the earlier article (Commer et al., 2001), the volcano is approximated by vertical conductive columns in a resistive fullspace that approximates air. The column scheme allows to accurately model topography. Furthermore, it is particularly useful if vertical conductivity changes dominate over lateral ones, as is the case for the layered structure indicated by the given a priori information. Refer to Commer (2003) for a more detailed description of the column model and related aspects such as FD grid stability.

Further a priori information arises from inversions of in–loop data (Koch, 2003) and LOTEM data (Kalscheuer et al., this issue) measured on profiles on the southern flank. The 1D interpretation results indicate a strong lateral resistivity variation which is interpreted as an assumed fault–like structure at the northern UTM coordinate 9159 km (Figure 2) in a 2D modeling approach shown by Kalscheuer et al. (this issue). Based on these results we choose the same location for a boundary, that extends infinitely into the west–east direction and allows different layered structures on both sides. The boundary is located at 7.2 km distance south from the summit. To its south three layers are allowed to vary, to the north we allow four layers. From several preliminary test inversions, which are not shown here, it could be concluded that this represents an optimum in terms of data fit and number of important parameters. More layers introduce less resolved parameters; less layers produce a worse data fit.

Figure 3 shows the inversion result after 12 Marquardt iterations. The model (a) both illustrates the parameterization and shows the final result. The initial parameter estimations given in brackets are based on the a priori information mentioned above. In spite of the small number of model parameters and the large area covered by the stations, a good data fit is obtained in general as shown by Figures 3b and c. Horizontal magnetic field time derivatives were measured at Stations 4–6, where Hx and Hy denote the field in a direction parallel and perpendicular to the transmitter, respectively.

An outstanding result is the very good fit of Station 7,

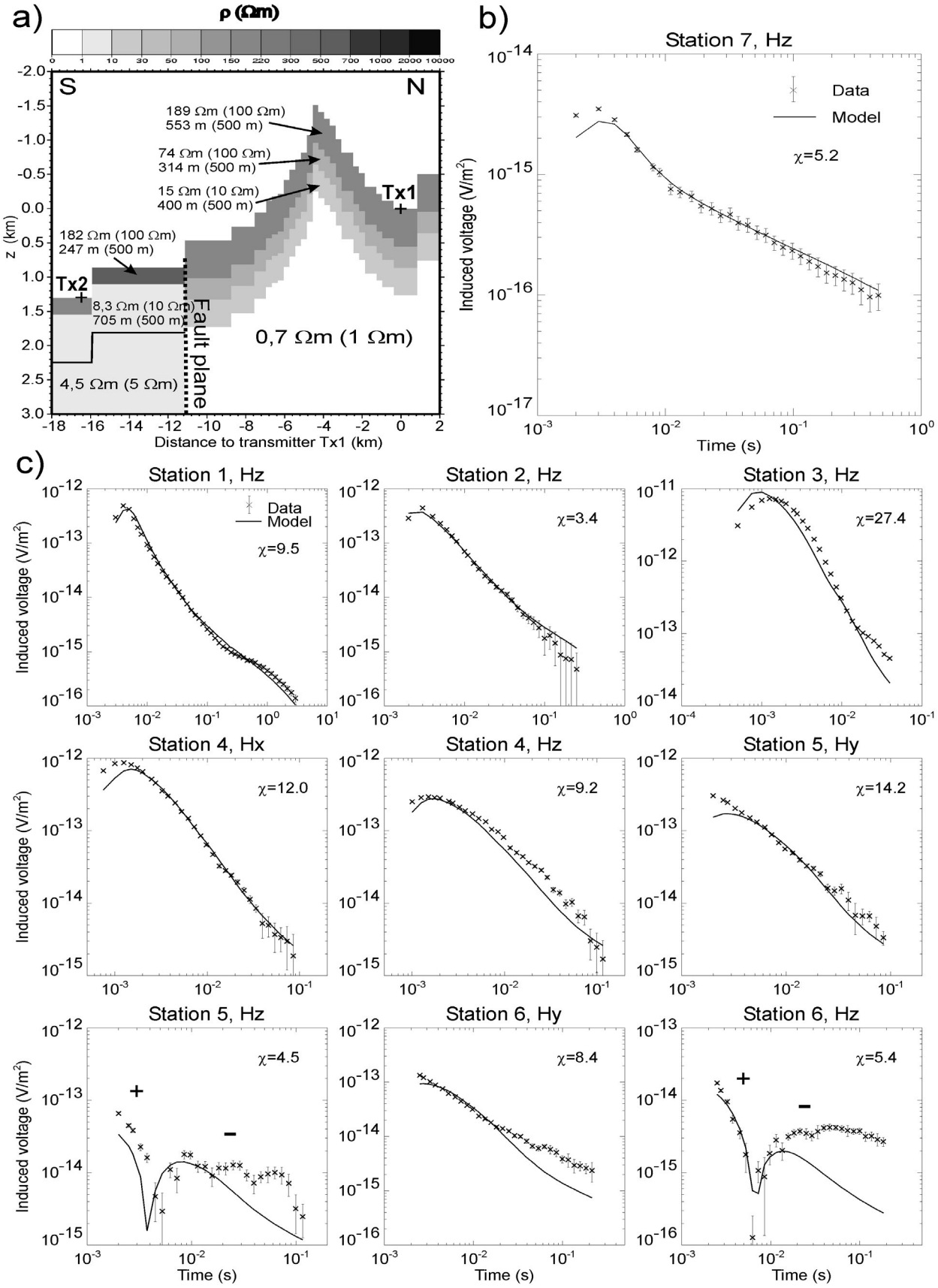

Figure 3: *Model results from a inversion of the combined data set including Stations 1–7 (see Figure 2) for a dome–shaped layered mountain model with a fault plane below the southern flank. (a) Final model result. (b) Final data fit for Station 7. (c) Final data fit for Stations 1–6.*

apart from the data before 3 ms, as this transient is generated by the southern transmitter. It shows that the transition to a more shallow good conductor in the south is essential for a fit. Without this additional model feature this transient cannot be reproduced by the layered model approach (Commer, 2003). In general, the data fit of Stations 1–6 can be regarded as good in a qualitative sense. The largest deviations are observed for Stations 5 and 6, indicating that more complex local anomalies are necessary for a further improvement of the fit.

Discussion

The presented inversion scheme may be regarded as a valid alternative for inversion problems that require models which are too complicated for a trial–and–error forward modeling, yet lack the amount of available data for a full large–scale inversion approach. The article has demonstrated that arbitrary 3D model parameters can be defined. Refer to Commer (2003) for examples of other types of parameters. Obviously, the necessity of a priori information for an appropriate parameterization is a major drawback. However, EM surveys often are conducted in addition to other geophysical disciplines providing structural information. We emphasize that the inversion scheme has been developed for cases where sufficient prior information is available. For cases lacking such information, a trial–and–error forward modeling is suggested to find suitable starting models which can be refined in an inversion.

Because of its low computational needs, the scheme represents a reasonable alternative to a large–scale 3D inversion. With a parallel computing platform[2] available, the shown field data example required a computation time of approximately three hours.

For the field data from the Merapi volcano, an improvement for a data interpretation is achieved by including the topography of the survey area. Because of acceptable qualitative data fits, a dome–shaped layering can be viewed as a good approximation of the general resisitivity structure over a scale outlined by the employed field configurations. The high basement conductivities are in general agreement with 1D LOTEM inversion results (Müller et al., 2002) and 3D MT modeling results (Müller, 2000) and support the hypothesis of a conductive hydrothermal system inside of the volcano (Zimmer and Erzinger, 1998). The clear transition to a different resistivity structure below the foothills of the southern flank indicates that conductivity sources may be different compard to the summit area as also proposed by Müller et al. (2002).

Acknowledgments

This work and the LOTEM surveys as part of the MERAPI project were supported by the German Science Foundation (DFG) (project number Ho1506/8-1). Vladimir Druskin and Leonid Knizhnerman allowed us to use their SLDM code. The field work at Merapi was undertaken with the help of 6 students from the University of Cologne and 10 students from the University of Bandung.

References

Alumbaugh, D. L., Newman, G. A., Prevost, L., and Shadid, J. N., 1996, Three-dimensional wideband electromagnetic modeling on massively parallel computers: Radio Science, **31**, 1–23.

Blohm, M., Hoekstra, P., and Blohm, R., 1991, Utility and limitations of 1–D inversions of time–domain EM data over strong 2–D structures:, 61st Ann. Internat. Mtg. and Exp., Soc. Expl. Geophys., Expanded abstracts, 410–411.

Christensen, N., 2002, A generic 1-D imaging method for transient electromagnetic data: Geophysics.

Commer, M., Hördt, A., and Helwig, S. L., 2001, 3D inversion of LOTEM data under strong boundary conditions, Protokoll über das Kolloquium elektromagnetische Tiefensondierung.

Commer, M., Helwig, S. L., and Tezkan, B., Untersuchungen zur Struktur des Vulkans Merapi (Zentral Java, Indonesien) mit transient elektromagnetischen Tiefensondierungen:, Abschlussbericht für das DFG–Projekt MERAPI, Teilprojekt LOTEM HO 1506/8–1, Univ. zu Köln, Inst. für Geophys. und Meteo., 2003.

Commer, M., 2003, Three–dimensional inversion of transient electromagnetic data: A comparative study: Doktorarbeit, Universität zu Köln.

Druskin, V. L., and Knizhnerman, L. A., 1988, A spectral semi-discrete method for the numerical solution of 3D-nonstationary problems in electrical prospecting: Physics of the solid Earth, **24**, 641–648.

Druskin, V., and Knizhnerman, L., 1994, Spectral approach to solving three–dimensional Maxwell's diffusion equations in the time and frequency domains: Radio Science, **29**, 937–953.

Druskin, V. L., Knizhnerman, L. A., and Lee, P., 1999, New spectral Lanczos decomposition method for induction modeling in arbitrary 3–D geometry: Geophysics, **64**, 701–706.

Friedel, S., Brunner, I., Jacobs, F., and Rücker, C., 2000, New results from DC resistivity imaging along the

[2]The presented inversions were calculated on 8 nodes of a SUN Fire 6800 computer.

flanks of Merapi Volcano *in* Zschau, J., and Westerhaus, M., Hrsg., Decade-Volcanoes under Investigation: Dt. Geophys. Gesellschaft, 23–29.

Gerstenecker, C., Läufer, G., Snitil, B., and Wrobel, B., 1998, Digital elevation models for Mount Merapi *in* Zschau, J., and Westerhaus, M., Hrsg., Decade-Volcanoes under Investigation: Dt. Geophys. Gesellschaft, 65–68.

Hördt, A., Druskin, V. L., and Knizhnerman, L. A., 1992, Interpretation of 3-D effects on long-offset transient electromagnetic (LOTEM) soundings in the Münsterland area / Germany: Geophysics, **57**, 1127–1137.

Hördt, A., Dautel, S., Tezkan, B., and Thern, H., 2000, Interpretation of long-offset transient electromagnetic data from the Odenwald area, Germany, using two-dimensional modelling: Geophys. J. Int., **140**, 577–586.

Hördt, A., 1989, Ein Verfahren zur 'Joint Inversion' angewandt auf 'Long Offset Electromagnetics' (LOTEM) und Magnetotellurik (MT): Diplomarbeit, Univ. zu Köln, Inst. für Geophys. und Meteo.

Hördt, A., 1998, Calculation of electromagnetic sensitivities in the time domain: Geophys. J. Int., **133**, 713–720.

Jackson, D. D., 1972, Interpretation of inaccurate, insufficient and inconsistent data: Geophys. J. R. astr. Soc., **28**, 97–109.

Jupp, D. L. B., and Vozoff, K., 1975, Stable iterative methods for the inversion of geophysical data: Geophys. J. R. astr. Soc., **42**, 957–976.

Koch, O., 2003, Transient–elektromagnetische Messungen zur Erkundung einer Leitfähigkeitsanomalie am Vulkan Merapi in Indonesien: Diplomarbeit, Univ. zu Köln, Inst. für Geophys. und Meteo.

Levenberg, K., 1944, A method for the solution of certain nonlinear problems in least squares: Quarterly of Applied Mathematics, **2**, 164–168.

Lines, L. R., and Treitel, S., 1984, Tutorial: A review of least-squares inversion and its application to geophysical problems: Geophys. Prospect., **32**, 159–186.

Madden, R., and Mackie, R. L., 1989, Three-Dimensional Magnetotelluric Modeling and Inversion: Proceedings of the IEEE, **77**, 318–333.

Marquardt, D. W., 1963, An algorithm for least-squares estimation of non-linear parameters: SIAM J., **11**, 431–441.

McGillivray, P. R., Oldenburg, D. W., Ellis, R. G., and Habashy, T. M., 1994, Calculating of sensitivities for the frequency-domain electromagnetic problem: Geophys. J. Int., **116**, 1–4.

Meju, M. A., 1994, Geophysical data analysis: Understanding inverse problem theory and practice:, 6 Society of Exploration Geophysicists, Tulsa.

Mitsuhata, Y., Uchida, T., and Amano, H., 2002, 2.5-D inversion of frequency–domain electromagnetic data generated by a grounded–wire source: Geophysics, **67**, 1753–1768.

Moskow, S., Druskin, V., Habashy, T., Lee, P., and Davydychewa, S., 1999, A finite difference scheme for elliptic equations with rough coefficients using a cartesian grid nonconforming to interfaces: SIAM J. Numerical Analysis, **36**, 442–464.

Müller, M., Hördt, A., and Neubauer, F. M., 2002, Internal structure of Mount Merapi, Indonesia, derived from long–offset transient electromagnetic data: J. Geophys. Res., **107**, ECV 2–1 – ECV 2–14.

Müller, A., 2000, Identification of good electric conductors below Merapi Volcano (Central Java) by magnetotellurics: DGG–Mitteilungen, Sonderband.

Newman, G. A., Anderson, W. L., and Hohmann, G. W., 1987, Interpretation of transient electromagnetic soundings over three–dimensional structure for the central–loop configuration: Geophys. J. R. astr. Soc., **89**, 889–914.

Petry, H., 1987, Transient elektromagnetische Tiefensondierungen — Modellrechnungen und Inversion: Diplomarbeit, Univ. zu Köln, Inst. für Geophys. und Meteo.

Scholl, C., Commer, M., Helwig, S. L., and Martin, R., 2002, LOTEM 3D Inversionen auf kleinen Linux–Clustern:, 62. Jahrestagung der Dt. Geophysik. Gesellsch. (Hannover), Tagungsband, 45–46.

Scholl, C., 2001, Die Periodizität von Sendesignalen bei Long-Offset Transient Electromagnetics: Diplomarbeit, Univ. zu Köln, Inst. für Geophys. und Meteo.

Smith, J. T., 1996, Conservative modeling of 3-D electromagnetic fields, Part II: Biconjugate gradient solution and an accelerator: Geophysics, **61**, 1319–1324.

Strack, K. M., 1992, Exploration with Deep Transient Electromagnetics: Elsevier, Amsterdam.

Taylor, K., Widmer, M., and Chesley, M., 1992, Use of transient electromagnetic to define local hydrogeology in an arid alluvial environment: Geophysics, **57**, 343–352.

Vozoff, K., and Jupp, D. L. B., 1975, Joint Inversion of Geophysical Data: Geophys. J. R. astr. Soc., **42**, 977–991.

Wang, T., Oristaglio, M., Tripp, A., and Hohmann, G., 1994, Inversion of diffusive transient elctromagnetic data by a conjugate–gradient method: Radio Science, **29**, 1143–1156.

Zhdanov, M. S., and Frenkel, M. A., 1983, The solution of inverse problems on the basis of the analytical continuation of the transient electromagnetic fields in the reverse time: J. Geomagn. Geoelectr., **35**, 747–765.

Zhdanov, M. S., and Wannamaker, P., 2002, Three-dimensional electromagnetics, Proceedings of the Second International Symposium: Elsevier-Verlag.

Zimmer, M., and Erzinger, J., 1998, Geochemical monitoring on Merapi Volcano, Indonesia *in* Zschau, J., and Westerhaus, M., Hrsg., Decade-Volcanoes under Investigation: Dt. Geophys. Gesellschaft, 89–92.

Zschau, J., Sukhyar, R., Purbawinata, M. A., Lühr, B., and Westerhaus, M., 1998, Project MERAPI — Interdisciplinary Research at a High-Risk Volcano *in* Zschau, J., and Westerhaus, M., Hrsg., Decade-Volcanoes under Investigation: Dt. Geophys. Gesellschaft, 3–8.